

# Monochloramine dissipation in storm sewer systems: field testing and model development

Qianyi Zhang, Mohamed Gaafar, Evan G. R. Davies, James R. Bolton and Yang Liu

## ABSTRACT

Monochloramine ( $\text{NH}_2\text{Cl}$ ), as the dominant disinfectant in drinking water chloramination, can provide long-term disinfection in distribution systems. However,  $\text{NH}_2\text{Cl}$  can also be discharged into storm sewer systems and cause stormwater contamination through outdoor tap water uses. In storm sewer systems,  $\text{NH}_2\text{Cl}$  dissipation can occur by three pathways: (i) auto-decomposition, (ii) chemical reaction with stormwater components, and (iii) biological dissipation. In this research, a field  $\text{NH}_2\text{Cl}$  dissipation test was conducted with continuous tap water discharge into a storm sewer. The results showed a fast decrease of  $\text{NH}_2\text{Cl}$  concentration from the discharge point to the sampling point at the beginning of the discharge period, while the rate of decrease decreased as time passed. Based on the various pathways involved in  $\text{NH}_2\text{Cl}$  decay and the field testing results, a kinetic model was developed. To describe the variation of the  $\text{NH}_2\text{Cl}$  dissipation rates during the field testing, a time coefficient  $f_T$  was introduced, and the relationship between  $f_T$  and time was determined. After calibration through the  $f_T$  coefficient, the kinetic model described the field  $\text{NH}_2\text{Cl}$  dissipation process well. The model developed in this research can assist in the regulation of tap water outdoor discharge and contribute to the protection of the aquatic environment.

**Key words** | field test, kinetic model, monochloramine dissipation, storm sewers

Qianyi Zhang  
Mohamed Gaafar  
Evan G. R. Davies  
James R. Bolton  
Yang Liu (corresponding author)  
Department of Civil and Environmental  
Engineering,  
University of Alberta,  
Edmonton, Alberta,  
Canada T6G 1H9  
E-mail: yang.liu@ualberta.ca

## INTRODUCTION

Monochloramine ( $\text{NH}_2\text{Cl}$ ) has been widely used as a drinking water secondary disinfectant because of its long-lasting disinfection ability (US EPA 2005; Wahman *et al.* 2009; Wahman & Speitel 2012). However,  $\text{NH}_2\text{Cl}$  can contaminate the aquatic environment when tap water is discharged into storm sewer systems. Several outdoor tap water use activities can introduce  $\text{NH}_2\text{Cl}$  into storm sewers, such as lawn irrigation, garden watering, individual car washing, driveway cleaning and industrial pressure vessel testing (Mayer *et al.*, 1999; Balling *et al.* 2008). To evaluate  $\text{NH}_2\text{Cl}$  concentrations in stormwater sewers, our previous studies collected and analyzed stormwater samples at different neighborhoods in Edmonton, Alberta, including residential and park locations with large garden and lawn areas, commercial locations, such as car dealerships and rentals, and industrial areas with fabricators of large pressure vessels. These field sampling results showed that during the summers of 2015 and 2016, the total active chlorine (TAC)

concentration in stormwater was as high as 0.77 mg/L (Zhang *et al.* 2018b), which exceeds the effluent discharge limit of 0.02 mg/L specified in the Canada-wide Strategy by the Canadian Council of Ministers of the Environment (CCME 2009). Compared with concentrated precipitation periods, the TAC concentrations were significantly higher in dry weather conditions (defined as low or no precipitation occurring during the sampling period).

Thus, monochloramine is the dominant active chlorine species in tap water, and tap water is the principal TAC source in storm sewers during dry weather. To protect water sources from TAC contamination,  $\text{NH}_2\text{Cl}$  dissipation mechanisms in storm sewer systems were studied. Three pathways that contribute to  $\text{NH}_2\text{Cl}$  decay are (i) auto-decomposition, (ii) chemical reactions with natural organic matter (NOM) and nitrate ( $\text{NO}_2^-$ ) in stormwater (Zhang *et al.* 2018a), and (iii) biological dissipation in the presence of storm sewer biofilms (Zhang 2018). The three

pathways have been studied previously (Zhang *et al.* 2017, 2018a; Zhang 2018).

In the present study, an  $\text{NH}_2\text{Cl}$  dissipation field test with continuous tap water discharge into storm sewer pipes in Edmonton was conducted. Further, a kinetics model was developed to simulate the three  $\text{NH}_2\text{Cl}$  decay pathways, with the field test results used to calibrate the model  $\text{NH}_2\text{Cl}$  decay parameters. The final model described the  $\text{NH}_2\text{Cl}$  decay process in storm sewers under various conditions and can be applied to estimate  $\text{NH}_2\text{Cl}$  consumption between discharge points and outfalls. This model is intended to contribute to governmental regulation of outdoor tap water uses, thus decreasing fresh water contamination by TAC species. It can be modified for regulation of tap water discharges by other cities concerned about  $\text{NH}_2\text{Cl}$  in their storm sewers.

## METHODS

### Site selection

The field  $\text{NH}_2\text{Cl}$  dissipation test was conducted in an uninterrupted storm sewer pipe (~200 m length) in a residential area in Edmonton. An uninterrupted pipe system was selected to eliminate the possibility of water flowing into or out of branch pipelines (Figure 1), while a residential area was selected because of its low traffic density and its potential  $\text{NH}_2\text{Cl}$  contamination through lawn irrigation and private car washing. The selected pipelines consisted of two pipe sections as shown in Figure 1.

### Storm sewer sediment and biofilm characterization

Biofilm samples were collected from storm sewer pipes by scraping biofilms within a 1.1 cm diameter template over a randomly-selected submerged pipe surface. Samples were stored in sterilized centrifuge tubes containing 5 mL of stormwater collected in the same sewer. Biofilm samples were kept on ice during transportation and preserved at 4 °C until they were analyzed. After samples were delivered to the laboratory, genomic DNA was extracted and *q*PCR was conducted to analyze the populations of total bacterial and ammonia-oxidizing bacteria (AOB) following methods reported previously (Zhang *et al.* 2018b). The total bacteria and AOB were analyzed by measuring *rpoB* and *amoA* functional genes. The primers used in *q*PCR analyses are shown in Table S1, available with the online version of this paper. In addition, volatile suspended solids (VSS)

were calculated following the Standard Methods 2540E protocol (AWWA/APHA/WEF 2012).

### Tap water quality analysis

The initial  $\text{NH}_2\text{Cl}$  concentrations were analyzed as soon as the samples were taken, to prevent any changes of  $\text{NH}_2\text{Cl}$  concentrations through the  $\text{NH}_2\text{Cl}$  auto-decomposition process. To aid  $\text{NH}_2\text{Cl}$  dissipation model development, other tap water characteristics such as pH, ammonium nitrogen ( $\text{NH}_4^+\text{-N}$ ), nitrite nitrogen ( $\text{NO}_2^-\text{-N}$ ), alkalinity, and NOM concentrations were measured after samples were delivered to the laboratory.

Since  $\text{NH}_2\text{Cl}$  is dominant in tap water, the  $\text{NH}_2\text{Cl}$  concentration was measured as the TAC concentration with the HACH (Loveland, USA) colorimetric method 8167 (detection limit 0.02 mg-Cl/L). The  $\text{NH}_4^+\text{-N}$  and alkalinity concentrations were analysed with HACH commercial test kits TNT832 and TNT870, respectively, with detection limits of 0.015 mg/L  $\text{NH}_3\text{-N}$  and 25 mg/L  $\text{CaCO}_3$ , respectively. The dissolved organic carbon (DOC) of tap water samples was measured with a Shimadzu TOC-L CPH E100 (detection limit 4 µg-C/L). The pH was determined with an Extech EC500 Waterproof ExStikII pH/conductivity meter (Extech Instruments, USA).

### Field $\text{NH}_2\text{Cl}$ dissipation test

During the field  $\text{NH}_2\text{Cl}$  dissipation study, tap water was released from a fire hydrant at point A (a curb inlet) for approximately 40 min. The tap water flowrate was adjusted to 10 L/s before discharge. 10 L/s was selected since it is closest to the stormwater flowrate under dry weather conditions. Time zero was recorded at point A upon introduction of tap water into the storm sewer. Thereafter, tap water samples were collected from the hydrant flow every 5 min from time zero using 250 mL chlorine free glass bottles, and the  $\text{NH}_2\text{Cl}$  concentrations in these water samples were analyzed. At point B, time zero was recorded when the first flow was observed at this point, and the first sample was collected at time 1 min. After that, samples were collected every 5 to 10 min from the same manhole.  $\text{NH}_2\text{Cl}$  concentrations were analysed immediately after sample collection to avoid the continuous reaction of  $\text{NH}_2\text{Cl}$  with stormwater chemical constitution in the samples. Moreover, dechloramination was conducted at point C and point D to prevent possible downstream  $\text{NH}_2\text{Cl}$  contamination, using commercial VITA-D-CHLOR tablets (Kent, USA).

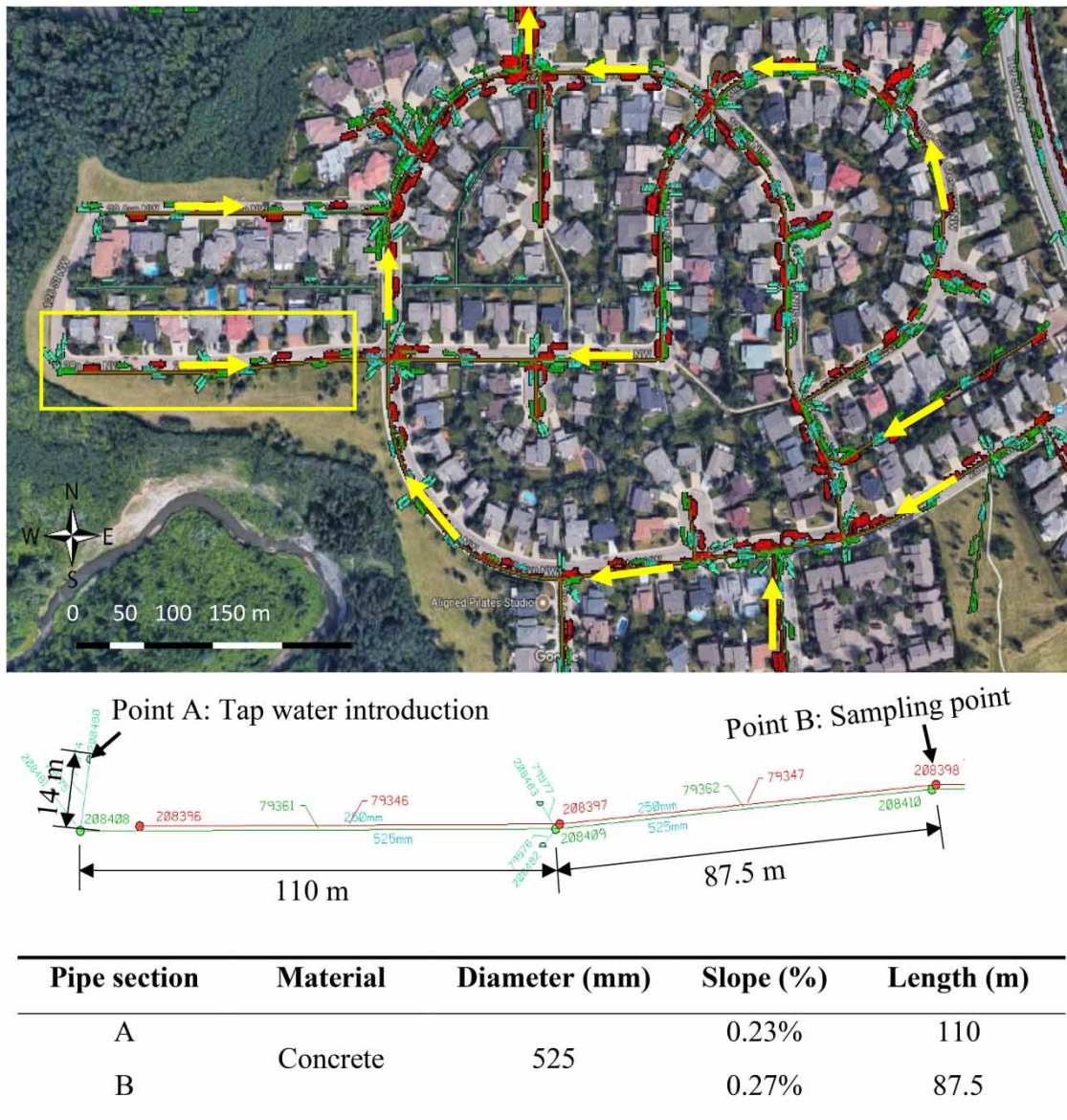


**Figure 1** | Plan views of storm sewer network at field  $\text{NH}_2\text{Cl}$  dissipation test location (yellow arrow: flow direction; green lines: storm sewer pipelines; red lines: sewage pipelines). The full color version of this figure is available in the online version of this paper, at <http://dx.doi.org/10.2166/wst.2018.512>.

## Model development

Figure 2 illustrates the kinetic reactions responsible for  $\text{NH}_2\text{Cl}$  dissipation in storm sewer systems, which is modified from our previous study (Zhang *et al.* 2017, 2018a; Zhang 2018). The reaction coefficients and equilibrium constants of these reactions are summarized in Table 1. The reactions involved in Figure 2 and Table 1 were developed from the literature and our previous research (Jafvert & Valentine 1992; Vikesland *et al.* 2001; Duirk *et al.* 2005; Wahman & Speitel 2012; Maestre *et al.* 2016; Zhang *et al.* 2017, 2018a; Zhang 2018).

Specifically, the  $\text{NH}_2\text{Cl}$  auto-decomposition kinetic model applied in this research was developed by Jafvert & Valentine (1992) and refined by Vikesland *et al.* (2001). The model also incorporates the reaction kinetics between  $\text{NH}_2\text{Cl}$  and  $\text{NO}_2^-$  developed by Margerum *et al.* (1994) and Vikesland *et al.* (2001), and the reactions between  $\text{NO}_2^-$  and the free chlorine released from  $\text{NH}_2\text{Cl}$ , as proposed by Wahman & Speitel (2012). Moreover, NOM is a dominant factor affecting  $\text{NH}_2\text{Cl}$  decay in bulk tap water and stormwater samples (Duirk *et al.* 2000, 2005; Zhang *et al.* 2017, 2018a; Zhang 2018); these  $\text{NH}_2\text{Cl}$  reactions with stormwater and tap water NOM, as described by Zhang *et al.* (2017) and

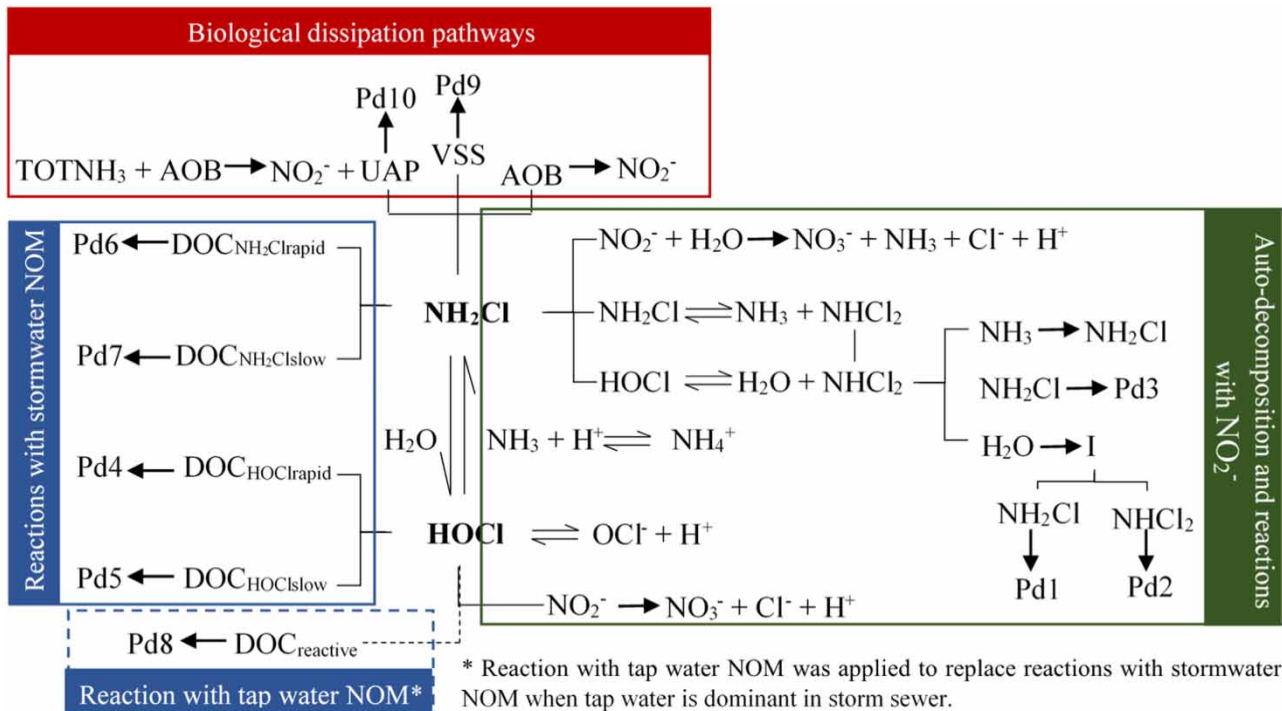


Figure 2 | Reactions involving  $\text{NH}_2\text{Cl}$  dissipation in a storm sewer system (Pd: products) (Zhang et al. 2017, 2018a; Zhang 2018).

Zhang et al. (2018a), were also included in the present model. The impacts of  $\text{Fe}^{2+}$  and  $\text{Br}^-$  were not included, since low concentrations were detected in our stormwater samples. Finally, storm sewer biofilm plays an important role in  $\text{NH}_2\text{Cl}$  dissipation, as it can react directly with  $\text{NH}_2\text{Cl}$  and consume  $\text{NH}_2\text{Cl}$  through AOB co-metabolism (Sathasivan et al. 2009; Maestre et al. 2013; Maestre et al. 2016). These biological dissipation mechanisms, as described by (Zhang 2018), were also included in the present model.

## RESULTS AND DISCUSSION

### Storm sewer and tap water characterization

To simulate  $\text{NH}_2\text{Cl}$  dissipation in storm sewer systems, the total biofilm concentrations and the AOB concentrations in storm sewer pipes were established (Table 2). The VSS concentrations (Table 2) represented the total biomass concentration in the biofilms. Since the water temperature was  $10^\circ\text{C}$  during the field test period, the modeled  $\text{NH}_2\text{Cl}$  decay rate was calibrated using a temperature coefficient developed in our previous studies (Zhang et al. 2017, Zhang 2018). Further, a time-dependent coefficient,  $f_T$ , was introduced to calibrate the modeled  $\text{NH}_2\text{Cl}$  dissipation rates for

various time intervals measured from time zero, called 'discharge times' here. The values of  $f_T$  under different discharge times,  $T$ , were solved based on field  $\text{NH}_2\text{Cl}$  dissipation tests. Before the field test, no flow was observed in the storm sewer pipes. Therefore, the impact of stormwater on  $\text{NH}_2\text{Cl}$  decay was not considered in this research.

### Chloramine dissipation in storm water sewers

Figure 3 shows the  $\text{NH}_2\text{Cl}$  concentration changes from the discharge point (point A) to the sampling point (point B) in the  $\text{NH}_2\text{Cl}$  decay field test, as well as the comparison of modeled and field results at point B. As shown in Figure 3(a), the initial  $\text{NH}_2\text{Cl}$  concentration at point A was slightly lower than the subsequent values, and increased to a stable level of approximately  $1.77\text{ mg active Cl/L}$ . The  $\text{NH}_2\text{Cl}$  concentration in the first sample showed a significant decrease at point B; and the extent of  $\text{NH}_2\text{Cl}$  decay reduced with the increase in discharge times. This observation indicates a decrease of  $\text{NH}_2\text{Cl}$  dissipation rate with increasing discharge time, which occurred because  $\text{NH}_2\text{Cl}$  consumed the biofilm and other reactive components in the sewer pipes as tap water flowed continuously into the storm sewer. In addition, under a flowrate of  $10\text{ L/s}$ , some biofilm may be sloughed from the pipes. As fewer reactive

**Table 1** | NH<sub>2</sub>Cl dissipation reactions expected in storm sewers (Jafvert & Valentine 1992; Vikesland *et al.*, 2001; Duirk *et al.* 2005; Wahman & Speitel 2012; Maestre *et al.* 2016; Zhang *et al.* 2017, 2018a; Zhang 2018)

	Reaction	Rate coefficient or equilibrium constant	References
<b>NH<sub>2</sub>Cl autodecomposition</b>			
1	HOCl + NH <sub>3</sub> → NH <sub>2</sub> Cl + H <sub>2</sub> O	$k_1 = 1.5 \times 10^{10} \text{ M}^{-1} \text{ h}^{-1}$	Morris & Isaac (1981)
2	NH <sub>2</sub> Cl + H <sub>2</sub> O → HOCl + NH <sub>3</sub>	$k_2 = 7.6 \times 10^{-2} \text{ h}^{-1}$	
3	HOCl + NH <sub>2</sub> Cl → NHCl <sub>2</sub> + H <sub>2</sub> O	$k_3 = 1.3 \times 10^6 \text{ M}^{-1} \text{ h}^{-1}$	
4	NH <sub>2</sub> Cl + H <sub>2</sub> O → HOCl + NH <sub>2</sub> Cl	$k_4 = 2.7 \times 10^{-3} \text{ h}^{-1}$	
5	2 NH <sub>2</sub> Cl → NHCl <sub>2</sub> + NH <sub>3</sub>	$k_5^a$	Jafvert & Valentine (1992)
6	NHCl <sub>2</sub> + NH <sub>3</sub> → 2 NH <sub>2</sub> Cl	$k_6 = 2.2 \times 10^8 \text{ M}^{-2} \text{ h}^{-1}$	Hand & Margerum (1983)
7	NHCl <sub>2</sub> + OH <sup>-</sup> → I	$k_7 = 4.0 \times 10^5 \text{ M}^{-1} \text{ h}^{-1}$	Jafvert & Valentine (1987)
8	NHCl <sub>2</sub> + I <sup>b</sup> → HOCl + pd1 <sup>c</sup>	$k_8 = 1.0 \times 10^8 \text{ M}^{-1} \text{ h}^{-1}$	Leao (1981)
9	NH <sub>2</sub> Cl + I → pd2 <sup>c</sup>	$k_9 = 3.0 \times 10^7 \text{ M}^{-1} \text{ h}^{-1}$	
10	NH <sub>2</sub> Cl + NHCl <sub>2</sub> → pd3 <sup>c</sup>	$k_{10} = 5.5 \text{ M}^{-1} \text{ h}^{-1}$	
11	HOCl = H <sup>+</sup> + OCl <sup>-</sup>	pK <sub>a</sub> = 7.5	Snoeyink & Jenkins (1980)
12	NH <sub>4</sub> <sup>+</sup> = NH <sub>3</sub> + H <sup>+</sup>	pK <sub>a</sub> = 9.3	
13	H <sub>2</sub> CO <sub>3</sub> = HCO <sub>3</sub> <sup>-</sup> + H <sup>+</sup>	pK <sub>a</sub> = 6.4	
14	HCO <sub>3</sub> <sup>-</sup> = CO <sub>3</sub> <sup>2-</sup> + H <sup>+</sup>	pK <sub>a</sub> = 10.3	
<b>Reactions with NO<sub>2</sub><sup>-</sup></b>			
15	HOCl + NO <sub>2</sub> <sup>-</sup> → H <sup>+</sup> + NO <sub>3</sub> <sup>-</sup> + Cl <sup>-</sup>	$k_{11}^d$	Margerum <i>et al.</i> (1994)
16	NH <sub>2</sub> Cl + NO <sub>2</sub> <sup>-</sup> + H <sub>2</sub> O → NH <sub>4</sub> <sup>+</sup> + NO <sub>3</sub> <sup>-</sup> + Cl <sup>-</sup> + H <sup>+</sup>	$k_{12}^e$	Wahman & Speitel (2012)
<b>Reactions with stormwater NOM</b>			
17	HOCl + DOC <sub>HOClrapid</sub> → pd4 <sup>f</sup>	$k_{13} = 2.3 \times 10^6 \text{ M}^{-1} \text{ h}^{-1}$	Zhang <i>et al.</i> (2018a)
18	HOCl + DOC <sub>HOClslow</sub> → pd5 <sup>f</sup>	$k_{14} = 3.9 \times 10^2 \text{ M}^{-1} \text{ h}^{-1}$	
19	NH <sub>2</sub> Cl + DOC <sub>NH2Clrapid</sub> → pd6 <sup>g</sup>	$k_{15} = 3.4 \times 10^4 \text{ M}^{-1} \text{ h}^{-1}$	
20	NH <sub>2</sub> Cl + DOC <sub>NH2Clslow</sub> → pd7 <sup>g</sup>	$k_{16} = 15.9 \text{ M}^{-1} \text{ h}^{-1}$	
<b>Reaction with tap water NOM</b>			
21	HOCl + DOC <sub>reactive</sub> → pd8 <sup>f</sup>	$k_{17} = 3.6 \times 10^6 \text{ M}^{-1} \text{ h}^{-1}$	Zhang <i>et al.</i> (2017)
<b>NH<sub>2</sub>Cl biological dissipation</b>			
22	NH <sub>3</sub> Monod: TOTNH <sub>3</sub> → NO <sub>2</sub> <sup>-</sup> + 0.062UAP	$k_{18}^h$	Zhang (2018)
23	Reaction with biofilm: NH <sub>2</sub> Cl + VSS <sup>i</sup> → pd9 <sup>g</sup>	$k_{19} = 2.5 \times 10^5 \text{ M}^{-1} \text{ h}^{-1}$	
24	Co-metabolism reaction: NH <sub>2</sub> Cl → NO <sub>2</sub> <sup>-</sup>	$k_{20} = 1.7 \text{ h}^{-1}$	
25	UPA reaction: NH <sub>2</sub> Cl + UAP → pd10 <sup>g</sup>	$k_{21} = 9.6 \times 10^5 \text{ M}^{-1} \text{ h}^{-1}$	

<sup>a</sup> $k_5 = k_H[H^+] + k_{HCO_3}[HCO_3^-] + k_{H_2CO_3}[H_2CO_3]$ , where  $k_H = 2.5 \times 10^7 \text{ M}^{-2} \text{ h}^{-1}$ ,  $k_{HCO_3} = 800 \text{ M}^{-2} \text{ h}^{-1}$ ,  $k_{H_2CO_3} = 4 \times 10^4 \text{ M}^{-2} \text{ h}^{-1}$ .

<sup>b</sup>I represents an unidentified intermediate in NH<sub>2</sub>Cl auto-decomposition.

<sup>c</sup>pd1-pd3 (pd means product) may include N<sub>2</sub>, H<sub>2</sub>O, Cl<sup>-</sup>, H<sup>+</sup>, NO<sub>3</sub><sup>-</sup> and other unidentified products (Jafvert & Valentine 1992).

$${}^d k_{11} = \frac{k_{1n}[H^+] \left(1 + \frac{k_{2n}[NO_2^-]}{K_{4n}}\right)}{\frac{k_{-1n}}{K_{4n}}[NH_3] + \left(1 + \frac{k_{2n}[NO_2^-]}{K_{4n}}\right)}, \text{ where } k_{1n} = 1.6 \times 10^8 \text{ M}^{-2} \text{ h}^{-1}, \frac{k_{-1n}}{K_{4n}} = 1.9 \times 10^6 \text{ M}^{-1}, \frac{k_{2n}}{K_{4n}} = 217 \text{ M}^{-1}.$$

$${}^e k_{12} = \frac{k_{1n'}[H^+] \left(1 + \frac{k_{2n}[NO_2^-]}{K_{4n}}\right)}{\frac{k_{-1n'}}{K_{4n}}[NH_3] + \left(1 + \frac{k_{2n}[NO_2^-]}{K_{4n}}\right)}, \text{ where } k_{1n'} = k_{Hn}[H^+] + k_{HCO_3n}[HCO_3^-] + k_{H_2CO_3n}[H_2CO_3], k_{Hn} = 4.3 \times 10^{10} \text{ M}^{-2} \text{ h}^{-1}, k_{HCO_3n} = 4.3 \times 10^3 \text{ M}^{-2} \text{ h}^{-1}, k_{H_2CO_3n} = 3.4 \times 10^6 \text{ M}^{-2} \text{ h}^{-1},$$

$$k_{-1n'}/K_{4n} = 2.1 \times 10^{-5} \text{ Mh} \times k_{1n'}.$$

<sup>f</sup>pd4-5, pd8 may include H<sub>2</sub>O, Cl<sup>-</sup>, H<sup>+</sup>, and chlorine disinfection by-products (DBPs).

<sup>g</sup>pd6-7, pd 9-10 may include NH<sub>4</sub><sup>+</sup>, H<sub>2</sub>O, Cl<sup>-</sup>, H<sup>+</sup>, and NH<sub>2</sub>Cl DBPs.

$${}^h k_{18} = \frac{1.8 \times 10^{-2} \times [AOB]}{6.1 \times 10^{-5} + \alpha[\text{TOTNH}_3]} \text{ mg} \cdot \text{TSSh}^{-1} \text{ L}^{-1}, [AOB] \text{ is considered to be constant, } \alpha \text{ is free ammonia to the TOTNH}_3 \text{ molar ratio.}$$

<sup>i</sup>The value of VSS used in this model is the VSS concentration (mg/L) divided by 156.9 based on the VSS consumption for each mole of NH<sub>2</sub>Cl.

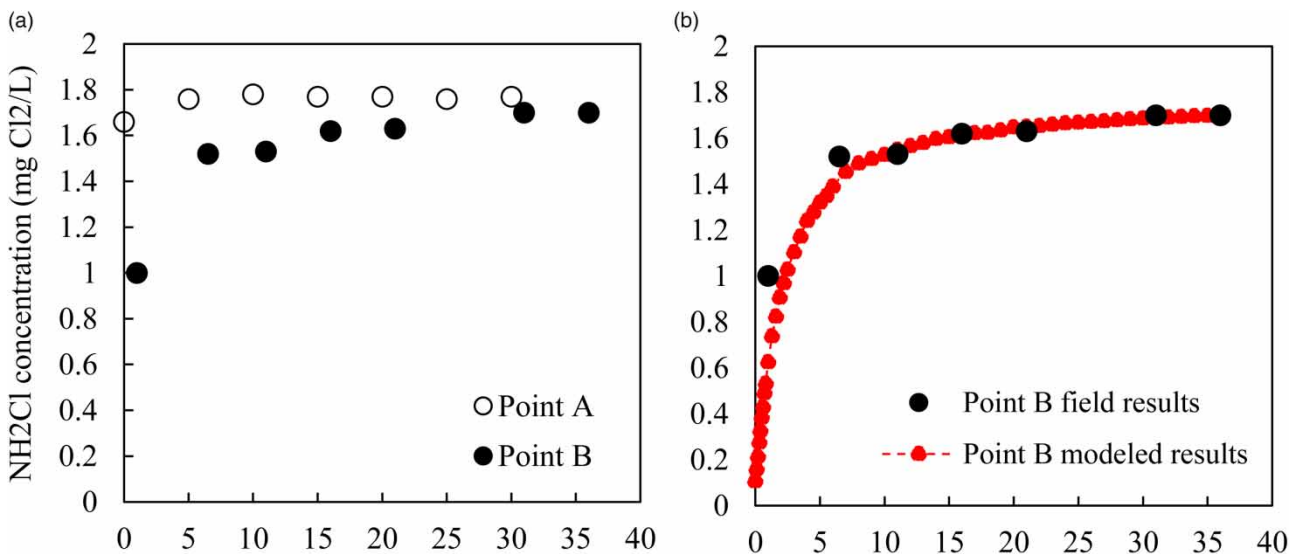
**Table 2** | Average values of model parameters for field NH<sub>2</sub>Cl decay tests in storm sewers (with standard errors)

	Model parameter	Measuring results
Pipe biofilm	Biomass per pipe surface area (mg/cm <sup>2</sup> )	8.06 ± 3.66
	Water biofilm contact ratio (cm <sup>2</sup> /L-water)	208
	Total bacterial functional gene (copies/cm <sup>2</sup> ) <sup>a</sup>	(1.33 ± 0.07) × 10 <sup>10</sup>
	Total biomass concentration (mg/L-water)	1,676 ± 746
	AOB functional gene (copies/cm <sup>2</sup> ) <sup>b</sup>	(5.31 ± 1.19) × 10 <sup>8</sup>
	AOB estimated concentration (mg/L-water)	27 ± 12
	Tap water flow	DOC (mg/L)
NH <sub>4</sub> <sup>+</sup> -N (mg/L)		0.390 ± 0.01
Alkalinity (mg CaCO <sub>3</sub> /L)		107 ± 7
pH		7.99 ± 0.01
Flow traveling time (points A to B, s)		420
Flowrate (L/s)		10

<sup>a</sup>Each bacterium is assumed to contain only one total bacterial functional gene (*rpoB* gene).

<sup>b</sup>Each AOB cell is assumed to contain an average of 2.5 *amoA* gene (He et al. 2007; Okano et al. 2004).

components remained in the storm sewer, the NH<sub>2</sub>Cl decay rate decreased. Figure 3(b) shows the simulated values at point B under the same conditions as the field test. The following sections provide a detailed discussion of modeled results.

**Figure 3** | NH<sub>2</sub>Cl concentration changes in storm sewer pipes with continuous tap water discharge: (a) field NH<sub>2</sub>Cl concentration changes in point A and B; (b) the comparison of modeled and field results at point B.

## Modeled monochloramine dissipation in storm water sewers

After the discharge of tap water at point A, it took 420 seconds (s) to arrive at point B. That is, for each flow, the modeled NH<sub>2</sub>Cl concentration at 420 s represents the residual NH<sub>2</sub>Cl concentration at point B. The NH<sub>2</sub>Cl decay rate of first flush (time zero) was firstly solved by the model (Figure 4, black line). After that, as reactive components in the storm sewers continuously reacted with NH<sub>2</sub>Cl and were flushed out by the tap water discharge, the NH<sub>2</sub>Cl decay rate gradually decreased.

To describe this NH<sub>2</sub>Cl decay rate variation under continuous discharge,  $f_T$  was introduced to calibrate the modeled results. The values of  $f_T$  under certain discharge times (1 min, 11 min, 21 min and 36 min) were solved based on the field NH<sub>2</sub>Cl dissipation rates from point A to point B, and the relationship between  $f_T$  and discharge times ( $T$ , min) can be described by the equation below ( $r^2 = 0.98$ ):

$$f_T = \frac{1}{1.73T + 1} \quad (1)$$

NH<sub>2</sub>Cl dissipation curves under time zero, 1 min, 11 min, 21 min and 36 min were then solved by the model and are shown in Figure 4. To verify the feasibility of this model, the field measured data that were not used for model calibration (field data collected at 6.5 min, 18 min and 31 min) were used to validate the model. Normalized Mean Square Error (NMSE) was added to describe the

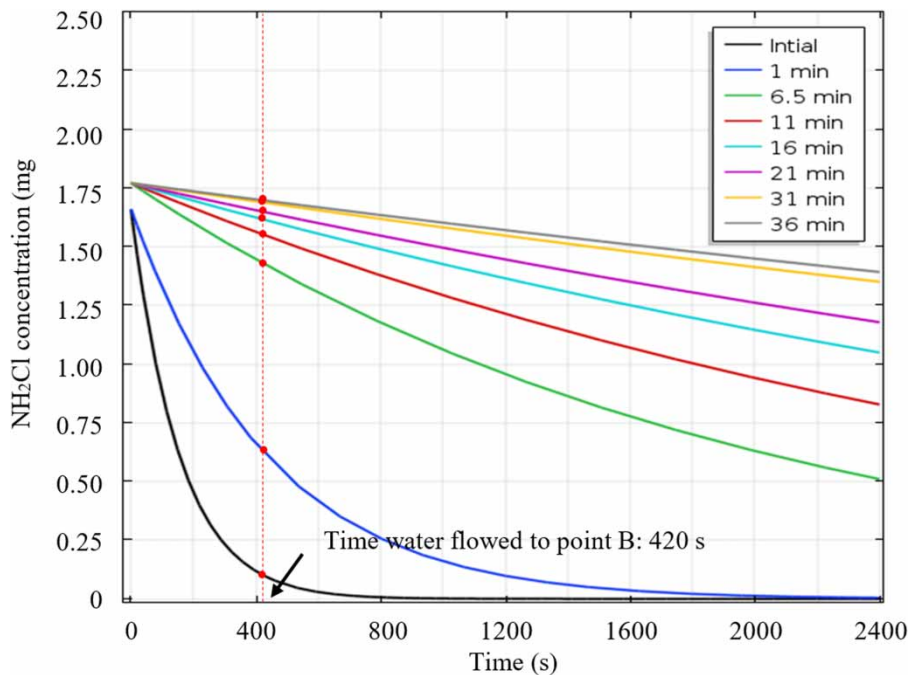


**Figure 4** | Modeled  $\text{NH}_2\text{Cl}$  dissipation with continuous tap water discharge at different discharge times (tap water discharge times are shown in the box at the top of the figure).

difference level between observed and modeled values. The expression of NMSE is defined below (Kusiak & Wei 2014):

$$NMSE = \frac{\sum_{i=1}^N (y_{ob} - y_{mod})^2}{\sum_{i=1}^N (y_{mod})^2} \quad (2)$$

where  $y_{ob}$  is the observed value from the field test at 6.5 min, 18 min and 31 min,  $y_{mod}$  is the predicted value from the model under same sampling times, and  $N$  is the number of analysis points.

In this study, the NMSE value = 0.001. This value was calculated based on the filed  $\text{NH}_2\text{Cl}$  data at 6.5 min, 18 min and 31 min and the correlated modeling results. With NMSE values no more than 0.015, the modeled and experimental data are considered to show good matches (Kusiak & Wei 2014). Therefore, the model developed in this research can simulate well the  $\text{NH}_2\text{Cl}$  dissipation process in storm sewer systems. Moreover, the comparison of modeled and field results at point B are shown in Figure 3(b). From this figure, modeling results and field data follows the same decay trend, and they show a good match at all the discharge times.

To further validate the calibrated model, the calibration process was repeated by randomly selecting another two groups of field data for model calibration (Group 2 and 3 in Table S2, available with the online version of this paper). Similar to the random selection Group 1, both

Groups 2 and 3 demonstrated the feasibility of the model (NMSE < 0.015). The detailed calibration results and NMSE values can be found in Supporting Information.

Figure 4 illustrates the tap water  $\text{NH}_2\text{Cl}$  dissipation rates in storm sewers for a number of discharge times. The initial  $\text{NH}_2\text{Cl}$  concentrations in the model were set at the field test values, and the discharge times represented by each colored line in the graph correspond to the sample collection times at point B. The vertical dashed line indicates the modeled  $\text{NH}_2\text{Cl}$  concentrations of each flow at point B. The  $\text{NH}_2\text{Cl}$  concentrations clearly increased at point B with later discharge times, and the rate of dissipation gradually reduced, which matches the field analysis results. Further, Figure 3(b) shows that the modeled  $\text{NH}_2\text{Cl}$  concentrations at 420 s (point B) correspond closely to the field testing results for the same discharge periods. Therefore, the model developed in this study accurately describes the  $\text{NH}_2\text{Cl}$  dissipation processes in Edmonton storm sewer systems under a continuous discharge condition.

## CONCLUSIONS

The  $\text{NH}_2\text{Cl}$  dissipation rate in storm sewer systems depends on pH, temperature, NOM and initial  $\text{NH}_2\text{Cl}$  concentrations, the biofilm population and storm sewer characteristics. Further, the  $\text{NH}_2\text{Cl}$  concentrations solved

by the calibrated model corresponded closely to the field results, which indicates that the model used in this research can simulate  $\text{NH}_2\text{Cl}$  dissipation rates in real storm sewers with continuous discharge.

With the model developed in this research, the  $\text{NH}_2\text{Cl}$  concentrations in storm sewer systems at the outfall points can be predicted under various outdoor tap water use activities. If the concentrations simulated by the model are higher than the discharge limit of  $0.02 \text{ mg-Cl}_2/\text{L}$ , additional measures such as stormwater dechloramination are required. Therefore, this model can be used for the regulations of tap water outdoor discharge and development of dechloramination plans, thus contributing to the protection of the natural environment.

## ACKNOWLEDGEMENTS

This research was supported by research funding from the Natural Sciences and Engineering Research Council of Canada (NSERC) and the City of Edmonton, Alberta, Canada.

## REFERENCES

- AWWA/APHA/WEF 2012 *Standard Methods for the Examination of Water and Wastewater*, 22nd edn. '2540 solids'. AWWA, Washington, DC, pp. 55–61.
- Balling, R. C., Gober, P. & Jones, N. 2008 *Sensitivity of residential water consumption to variations in climate: an intraurban analysis of Phoenix, Arizona*. *Water Resources Research* **44** (10), W10401.
- Canadian Council of Ministers of the Environment 2009 Canada-wide strategy for the management of municipal wastewater effluent, Winnipeg. [http://www.ccme.ca/files/Resources/municipal\\_wastewater\\_effluent/cda\\_wide\\_strategy\\_mwwe\\_final\\_e.pdf](http://www.ccme.ca/files/Resources/municipal_wastewater_effluent/cda_wide_strategy_mwwe_final_e.pdf) (accessed 28 November 2017).
- Duirk, S. E., Gombert, B., Choi, J. & Valentine, R. L. 2002 *Monochloramine loss in the presence of humic acid*. *Journal of Environmental Monitoring* **4** (1), 85–89.
- Duirk, S. E., Gombert, B., Croué, J. P. & Valentine, R. L. 2005 *Modeling monochloramine loss in the presence of natural organic matter*. *Water Research* **39** (14), 3418–3431.
- Hand, V. C. & Margerum, D. W. 1983 *Kinetics and mechanisms of the decomposition of dichloramine in aqueous solution*. *Inorganic Chemistry* **22**, 1449–1456.
- He, J. Z., Shen, J. P., Zhang, L. M., Zhu, Y. G., Zheng, Y. M., Xu, M. G. & Di, H. 2007 *Quantitative analyses of the abundance and composition of ammonia-oxidizing bacteria and ammonia-oxidizing archaea of a Chinese upland red soil under long-term fertilization practices*. *Environmental Microbiology* **9** (9), 2364–2374.
- Jafvert, C. T. & Valentine, R. L. 1987 *Dichloramine decomposition in the presence of excess ammonia*. *Water Research* **21** (8), 967–973.
- Jafvert, C. T. & Valentine, R. L. 1992 *Reaction scheme for the chlorination of ammoniacal water*. *Environmental Science and Technology* **26** (3), 577–586.
- Kusiak, A. & Wei, X. 2014 *Prediction of methane production in wastewater treatment facility: a data-mining approach*. *Annals of Operations Research* **216** (1), 71–81.
- Leao, N. I. 1981 *Kinetics of Combined Chlorine: Reactions of Substitution and Redox*. PhD Dissertation, University of California, Berkeley, CA.
- Maestre, J. P., Wahman, D. G. & Speitel, G. E. 2013 *Monochloramine cometabolism by *Nitrosomonas europaea* under drinking water conditions*. *Water Research* **47** (13), 4701–4709.
- Maestre, J. P., Wahman, D. G. & Speitel, G. E. 2016 *Monochloramine cometabolism by mixed-culture nitrifiers under drinking water conditions*. *Environmental Science and Technology* **50** (12), 6240–6248.
- Margerum, D. W., Schurter, L. M., Hobson, J. & Moore, E. E. 1994 *Water chlorination chemistry: Nonmetal redox kinetics of chloramine and nitrite ion*. *Environmental Science and Technology* **28** (2), 331–337.
- Mayer, P. W., Deoreo, W. B., Opitz, E. M., Kiefer, J. C., Davis, W. Y., Dziegielewski, B. & Nelson, J. O. 1999 Residential end uses of water. In: *Water Engineering and Management* **310**, xxi–xxxvii. AWWA Research Foundation/American Water Works Association, Washington, DC.
- Morris, J. C. & Isaac, R. A. 1981 *A critical review of kinetic and thermodynamic constants for the aqueous chlorine-ammonia system*. In: *Water Chlorination: Environmental Impact and Health Effects* (V. A. J. R. L. Jolley, W. A. Brungs, J. A. Cotruvo, R. B. Cumming & J. S. Mattice, eds). Arbor Science, Ann Arbor, MI, pp. 49–62.
- Okano, Y., Hristova, K. R., Leutenegger, C. M., Jackson, L. E., Denison, R. F., Gebreyesus, B., Lebauer, D. & Scow, K. M. 2004 *Application of real-time PCR to study effects of ammonium on population size of ammonia-oxidizing bacteria in soil*. *Applied and Environmental Microbiology* **70** (2) 1008–1016.
- Sathasivan, A., Chiang, J. & Nolan, P. 2009 *Temperature dependence of chemical and microbiological chloramine decay in bulk waters of distribution system*. *Water Science and Technology: Water Supply* **9** (5), 493–499.
- Noeyink, V. & Jenkins, D. 1980 *Water Chemistry*. Wiley, New York, NY.
- US EPA Office of Water, Office of Ground Water and Drinking Water, and Drinking Water Protection Division 2005 *Economic Analysis for the Final Stage 2 Disinfectants and Disinfection Byproducts Rule*. US EPA, Washington, DC.
- Vikesland, P. J., Ozekin, K. & Valentine, R. L. 2001 *Monochloramine decay in model and distribution system waters*. *Water Research* **35** (7), 1766–1776.
- Wahman, D. G. & Speitel, G. E. 2012 *Relative importance of nitrite oxidation by hypochlorous acid under chloramination conditions*. *Environmental Science and Technology* **46** (11), 6056–6064.

- Wahman, D. G., Wulfeck-Kleier, K. A. & Pressman, J. G. 2009 Monochloramine disinfection kinetics of *Nitrosomonas europaea* using propidium monoazide quantitative PCR and Live/Dead BacLight Methods. *Applied and Environmental Microbiology* **75** (17), 5555–5562. [http://www.ncbi.nlm.nih.gov/entrez/query.fcgi?cmd=Retrieve&db=PubMed&dopt=Citation&list\\_uids=19561179](http://www.ncbi.nlm.nih.gov/entrez/query.fcgi?cmd=Retrieve&db=PubMed&dopt=Citation&list_uids=19561179).
- Zhang, Q. 2018 Monochloramine Dissipation Mechanisms in Storm Sewer Systems. PhD Dissertation, University of Alberta, Edmonton, AB, Canada, pp. 122–148.
- Zhang, Q., Davies, E. G. R., Bolton, J. & Liu, Y. 2017 Monochloramine loss mechanisms in tap water. *Water Environment Research* **89** (11), 1999–2005.
- Zhang, Q., Davies, E. G. R., Bolton, J. R. & Liu, Y. 2018a Monochloramine loss mechanisms and dissolved organic matter characterization in stormwater. *Science of the Total Environment* **631–632**, 745–754.
- Zhang, Q., Gaafar, M., Yang, R. C., Ding, C., Davies, E. G. R., Bolton, J. R. & Liu, Y. 2018b Field data analysis of active chlorine-containing stormwater samples. *Journal of Environmental Management* **206**, 51–59.

First received 17 July 2018; accepted in revised form 5 December 2018. Available online 14 December 2018